The Southern Ocean: A Ventilation Contributor with Multiple Sources

Hartmut H. Hellmer and Aike Beckmann

Alfred-Wegener-Institute for Polar and Marine Research, Bremerhaven, Germany

Abstract.
Based on water mass analysis, the Weddell Sea in the Atlantic sector was identified as the major source for Southern Ocean bottom water. Recent observations, and tracer analysis and modeling indicate that the Indian-Pacific sector might be the location of additional bottom water sources similar in magnitude as their Atlantic counterpart. Numerical model results presented here suggest that the Atlantic and Indian-Pacific contributions to Southern Ocean bottom water are roughly equal but for waters of different density. The observationally derived formation rate of dense Antarctic Bottom Water of the order of 10 Sv (1 Sv = 10^6 m^3 s^{-1}) is confirmed by the model results but doubles if the lighter component of the Indian-Pacific sector is included. This result suggests that southern and northern hemisphere sources are equal contributors to the ventilation of the deep world ocean.

Introduction

The discussion concerning the production of Southern Ocean deep water was recently revived by different estimates based on global [*Broecker et al.,* 1998; *Broecker et al.,* 1999] and southern hemisphere [*Orsi et al.,* 1999] tracer distributions. Using the tracers PO_4^* and radiocarbon, the former required a centennial mean southern deep water formation rate similar to that of North Atlantic Deep Water (∼15 Sv). However, based on CFC-11 inventories for the deep Southern Ocean this estimate has been reduced drastically for the 20^{th} century pointing to higher formation rates during the Little Ice Age [*Broecker et al.,* 1999]. Since it was estimated to provide ∼ 70% of the total Antarctic Bottom Water (AABW) in the Southern Ocean [*Carmack,* 1977], past hydrographic observations were mainly focused on the Weddell Sea. There, formation rates of newly formed bottom water range from 1-5 Sv but increase up to 11 Sv if the formation of deep water is also considered (*Meredith et al.* [2001], and references therein). A circumpolar bottom water production rate has recently been corroborated by a Southern Ocean CFC-11 study which provides a total Antarctic Bottom Water formation rate of

8-9.5 Sv with 60% attributed to the Atlantic and 40% to the Indian-Pacific sectors [*Orsi et al.,* 1999]. The reasons for the discrepancies between the various estimates might be manifold: (1) the temporal variability of bottom water formation occurs on timescales longer than the period covered by modern hydrographic observations; (2) multiple (undetected) bottom water sources and spreading paths exist around and off Antarctica; (3) the techniques applied still contain uncertainties; (4) the estimates lack a common definition of the water mass characteristics ventilating the deep world ocean.

Measurements at high spatial and temporal resolution covering the entire Antarctic shelf regime are currently not feasible. Only recently, field experiments started to focus on the deep water transport across the ocean ridges confining the Weddell Sea to the north and east [*Haine et al.,* 1998; *Gordon et al.,* 2001]. Consequently, the most readily available and convenient tool able to provide additional information on deep and bottom water formation in the Southern Ocean is a numerical model with a resolution high enough to capture the controlling features of bottom topography, and with the physics detailed enough to describe air-sea ice/ice shelf-ocean interaction, deep convection and the nonlinear processes related to bottom water formation at the continental margin.

In the framework of BRIOS (Bremerhaven Regional Ice Ocean Simulations) we run a model with a horizontal resolution of 20-100 km in the Weddell Sea sector, embedded in a coarser circumpolar Southern Ocean, and a vertical resolution of 24 terrain-following levels [*Beckmann et al.,* 1999]. The model domain extends from 82°S to 50°S where temperature and salinity fields are strongly restored to the climatology of the Hydrographic Atlas of the Southern Ocean [*Olbers et al.,* 1992]. BRIOS represents the first OGCM to include all major Antarctic ice shelf cavities and the processes at the ice shelf base [*Hellmer et al.,* 1998]. BRIOS is forced with averaged monthly mean surface fluxes of momentum and freshwater, all resulting from a standalone sea ice model (after *Lemke et al.* [1990]). The latter is driven with 6-hourly ECMWF reanalysis data of the period 1985-93. The model successfully reproduces the present-day large scale ocean circulation and water mass structure of the Southern Ocean [*Beckmann et al.,* 1999]. Our analysis concentrates on the zonally (circumpolar) integrated overturning transport streamfunction plotted as a function of latitude and density (σ_2). This presentation is preferred to latitude and depth, because most of the water masses are modified at the same latitude and within the same depth

range as they move with the southern branches of the subpolar gyres. Therefore, the overturning rate of the southern cell often appears to be quite weak (3-5 Sv) in latitude versus depth presentations (e.g., *Häkkinen* [1995]). The density was chosen relative to 2000 meters to present an isopycnal range which coincides with *Orsi et al.'s* [1999] density based definition of AABW formed south of the Antarctic Circumpolar Current (ACC), $\sigma_2 \geq 37.16$ kg m^{-3}.

Results

The Southern Ocean is dominated by two meridional overturning cells which differ in orientation and density range (Fig. 1). Within the southern cell (counterclockwise in this figure), water masses with densities $\sigma_2 \geq 37.15$ kg m^{-3} are formed at a rate of approximately 21 Sv. This rate reduces to 11 Sv for bottom water denser $\sigma_2 \geq 37.16$ kg m^{-3}. Flowing north across 62°S, both dense water masses gain buoyancy due to mixing with Circumpolar Deep Water (CDW) as they enter the ACC region, defined by the position of the southern ACC front with a circumpolar mean of ~ 60°S [*Orsi et al.,* 1995]. The circumpolar integral implies weak southward flow near the bottom north of 62°S. This might be an artifact caused by the presence of the northern model boundary at 50°S. The recirculating (upper) branch of the southern cell reaches near-surface levels on the Antarctic continental shelf. The densest surface and bottom waters are both found here. The transition toward lighter surface waters at 78°S corresponds to the ice shelf edges, where shelf water modified by brine release from sea ice formation encounters waters carrying glacial meltwater from ice shelf basal melting.

A notable feature of the northern cell (clockwise circulation), representing the southern extension of the ACC, is the CDW's buoyancy gain between 58°S and 64°S (Fig. 1). Although not as abrupt as a circumpolar integration might suggest, CDW gradually changes characteristics eastward from the Atlantic due to continuous mixing with lighter surface waters. The modeled horizontal surface density distribution reveals the biggest change occurring in the eastern Pacific sector (not shown).

The horizontal distribution of near-bottom density shows that the ocean basins surrounding Antarctica are filled with AABW originating from the western continental shelves of Weddell and Ross seas (Fig. 2). Supply from the latter occurs through a narrow band while dense waters on the continental shelf off Wilkes-Adélie to Enderby Lands do not reach the abyssal ocean. This

is a result of the annual-mean presentation which hides bottom water formation during early winter in this region. AABW extends in a layer up to 1000 m thick to the northern model boundary in the western South Atlantic and Indian oceans.

Separation of the Southern Ocean into Atlantic and Indian-Pacific sectors south of 66°S shows that the densest water is found close to and beneath the Ross Ice Shelf (Fig. 3). However, this dense water does not reach the deep basins. Instead, the densest water crossing 66°S originates from the southern Weddell Sea continental slope (Fig. 3) resulting from mixing of ice shelf cavity outflow with deep water. Between 72°S and 66°S the density of this water mass increases indicating the admixture of waters from the western Weddell Sea continental shelf. The latter also produces a lighter type of AABW still denser than bottom water formed in the Indian-Pacific sector. Here, the admixture of lighter bottom water in a similar latitudinal band (compare maximum densities in Fig. 3) seems to erase the high-density signal of the Ross Sea outflow. Considering a slightly broader definition for AABW, $\sigma_2 \geq 37.15$ kg m^{-3}, both sectors combine sources of roughly equal strength (~ 10 Sv).

Discussion

In agreement with observations [*Carmack,* 1977; *Mantyla and Reid,* 1983], our model results show that the Southern Ocean has multiple bottom water sources. With a clear spatial division, they produce bottom water of different density at a total rate of ~ 20 Sv pointing to a southern source of equal strength as its northern hemisphere counterpart. The circumpolar integration (Fig. 1) implies no export of these water masses beyond 50°S but mixing with CDW and upwelling to the near-surface. However, a thick (~ 1000 m) layer of dense AABW combined with northerly flow exists in the Atlantic and Indian sectors indicating the export routes to the ocean basins beyond the model domain.

Most of the dense ($\sigma_2 \geq 37.16$ kg m^{-3}) AABW is formed in the Atlantic sector at an annual mean rate of ~ 10 Sv. This is twice the amount inferred from the circumpolar tracer budget and corresponds to the total Southern Ocean production rate [*Orsi et al.,* 1999]. However, the model's seasonal variability ranges from 7 Sv in summer to 11 Sv in winter, and interannual variability as observed by *Fahrbach et al.* [2001] is not accounted for in the model forcing. In addition, less dense bottom water might form off the southern Weddell Sea continental shelf since the mid-80's due to the disturbance of the shelf regime by stranded icebergs [*Grosfeld*

et al., 2001]. Finally, the CFC analysis might bear some uncertainties, e.g., due to insufficient station coverage in the source regions, which could post the derived range as a lower estimate.

A sligtly lighter ($\sigma_2 \geq 37.15$ kg m^{-3}) AABW is formed in the Indian-Pacific sector also at an annual mean rate of $\sim$ 10 Sv. The density difference results from the less dense parent water masses at the formation site, i.e., the continental shelf break/slope as the comparison of minimum and maximum densities north of 74°S shows (Fig. 3). The Southern Ocean's densest water exists in the inner Ross Sea, but it rapidly vanishes towards the north as it encounters the lighter waters off the continental shelf. The density increase combined with the formation of dense AABW at a rate of $\sim$ 3 Sv north of 68°S could correspond to the continental slopes off Adélie Land [*Rintoul,* 1998] and/or Prydz Bay [*Jacobs and Georgi,* 1977; *Schodlok et al.,* 2001]. In contrast to the formation of lighter AABW, the dense AABW formation is subject to seasonal variability ranging from from 2 Sv in summer to 5 Sv in winter. Although the dense AABW vanishes north of 66°S (Fig. 3), indicating enhanced mixing with ambient lighter water masses, the Indian sector produces between 20% (summer) and 30% (winter) of the Southern Ocean's dense AABW. This agrees well with the ratio of 72% estimated for the Weddell Sea/Atlantic sector [*Carmack,* 1977].

The horizontal bottom density distribution (Fig. 2) indicates that dense shelf water masses are not formed on the eastern Pacific continental shelves. But they are discharged continuously to the deep ocean basins in western Weddell and Ross seas and intermittent (not shown) along the shelf off Wilkes-Adélie toward Enderby lands as observed, e.g., off Adélie Land by *Fukamachi et al.* [2000]. Trapping by the coastal current was considered as a possible process for increasing shelf water salinities in the Indian sector and the current's relaxation as a possible period for dense water outflow and the formation of lighter bottom water [*Gordon,* 1974].

Our results emphasize that the apparent discrepancy between global and regional estimates of bottom water formation might be caused by a limited view of which water masses comprise ventilated components. Especially in the Weddell Sea, deep and bottom waters seem to carry different amounts of waters which recently were in contact with the atmosphere [*Gordon et al.,* 2001]. While Weddell Sea Bottom Water certainly is the densest, newly ventilated water mass formed at the southwestern continental slope [*Gordon,* 1998], it can be

transferred to the global ocean only by mixing with overlaying waters. In our model, the mixing and the transfer to shallower levels occur within the southern overturning cell. However, the broad density range in the deep Weddell Sea and the lower densities in the deep Indian-Pacific sector (Fig. 3) suggest that newly formed mixtures are injected (directly) at shallower levels along isopycnals which cross the basin confining mid-ocean ridges.

The model results presented here (and in *Beckmann et al.* [1999]) support the results of numerous field observations. Therefore, the BRIOS model family seems to be a valuable tool for investigating processes and their variabilities in the Southern Ocean. We expect that future modifications will cause regional improvements, especially in the Indian-Pacific sector, but will not change the large-scale picture: multiple sources in the Southern Ocean contribute to the deep and bottom waters of the world ocean at rates similar to their northern counterpart.

Acknowledgments. We are greatful to the members of the BRIOS group, especially to R. Timmermann and M. Schodlok, for their contributions, to M. England, S. Jacobs, P. Schlosser, and four anonymous reviewers for their comments which significantly improved the original manuscript.

References

Beckmann, A., H. H. Hellmer, and R. Timmermann, A numerical model of the Weddell Sea: Large scale circulation and water mass distribution, *J. Geophys. Res.*, *104*, 23,375-23,391, 1999.

Broecker, W. S., S. Sutherland, and T.-H. Peng, A possible 20th-century slowdown of Southern Ocean deep water formation, *Science*, *286*, 1132-1135, 1999.

Broecker, W. S., S. L. Peacock, S. Walker, R. Weiss, E. Fahrbach, M. Schröder, U. Mikolajewicz, C. Heinze, R. Key, T.-H. Peng, and S. Rubin, How much deep water is formed in the Southern Ocean, *J. Geophys. Res.*, *103*, 15,833-15,843, 1998.

Carmack, E. C., Water characteristics of the Southern Ocean south of the Polar Front, in *A Voyage of Discovery, George Deacon 70^{th} Anniversary Volume,* edited by M. Angel, pp. 15-41, Pergamon Press, Oxford, 1977.

Fahrbach, E., S. Harms, G. Rohardt, M. Schröder, and R. Woodgate, Flow of bottom water in the northwestern Weddell Sea, *J. Geophys. Res.*, *106*, 2761-2778, 2001.

Fukamachi, Y., M. Wakatsuchi, K. Taira, S. Kitagawa, S. Ushio, A. Takahashi, K. Oikawa, T. Furukawa, H. Yoritaka, M. Fukuchi, and T. Yamanouchi, Seasonal variability of bottom water properties off Adélie Land, Antarctica, *J. Geophys. Res.*, *105*, 6531-6540, 2000.

Gordon, A. L., Varieties and variability of Antarctic Bottom Water, *Colloques Internationaux du C.N.R.S.*, N°215, Processus de Formation des Eaux Océaniques Profondes, 1974.

Gordon, A. L., Western Weddell Sea thermohaline stratification, in *Ocean, Ice, and Atmosphere,* edited by S. S. Jacobs and R. F. Weiss, Antarctic Res. Ser. *75,* pp. 215-240, AGU, Washington DC, 1998.

Gordon, A. L., M. Visbeck, and B. Huber, Export of Weddell Sea Deep and Bottom Water, *J. Geophys. Res.*, *106*, 9005-9018, 2001.

Grosfeld, K., M. Schröder, E. Fahrbach, R. Gerdes, and A. Mackensen, How iceberg calving and grounding change the circulation and hydrography in the Filchner Ice Shelf/ocean system, *J. Geophys. Res.*, *106*, 9039-9056, 2001.

Haine, T. W. N., A. J. Watson, M. I. Liddicoat, and R. R. Dickson, The flow of Antarctic bottom water to the southwest Indian Ocean estimated using CFCs, *J. Geophys. Res.*, *103*, 27,637-27,653, 1998.

Häkkinen, S., Seasonal simulation of the Southern Ocean coupled ice-ocean system, *J. Geophys. Res.*, *100*, 22,733-22,748, 1995.

Hellmer, H. H., S. S. Jacobs, and A. Jenkins, Oceanic erosion of a floating Antarctic glacier in the Amundsen Sea, in *Ocean, Ice, and Atmosphere,* edited by S. S. Jacobs and R. F. Weiss, Antarctic Res. Ser. *75,* pp. 83-99, AGU, Washington DC, 1998.

Jacobs, S. S., and D. T. Georgi, Observations in the southwest Indian/Antarctic ocean, in *A Voyage of Discovery,* edited by M. V. Angel, Suppl. to Deep-Sea Res., *24,* 43-89, 1977.

Lemke, P., W. B. Owens, and W. D. Hibler III, A coupled sea ice-mixed layer-pycnocline model for the Weddell Sea, *J. Geophys. Res.*, *95*, 9513-9525, 1990.

Mantyla, A. W., and J. L. Reid, Abyssal characteristics

of the World Ocean waters, *Deep Sea Res.*, *30*, 805-833, 1983.

Meredith, M. P., A. J. Watson, K. A. Van Scoy, and T. W. N. Haine, Chorofluorocarbon-derived formation rates of the deep and bottom waters of the Weddell Sea, *J. Geophys. Res.*, *106*, 2899-2919, 2001.

Olbers, D. J., V. Gouretski, G. Seiß, and J. Schröter, *Hydrographic Atlas of the Southern Ocean,* 82pp., Alfred Wegener Institute, Bremerhaven, Germany, 1992.

Orsi, A. H., T. Whitworth III, and W. D. Nowlin Jr., On the meridional extent and fronts of Antarctic Circumpolar Current, *Deep Sea Res.*, *42*, 641-673, 1995..

Orsi, A. H., G. C. Johnson, and J. L. Bullister, Circulation, mixing, and production of Antarctic Bottom Water, *Prog. Oceanogr., 43,* 55-109, 1999.

Rintoul, S. R., On the origin and influence of Adélie Land bottom water, in *Ocean, Ice, and Atmosphere,* edited by S. S. Jacobs and R. F. Weiss, Antarctic Res. Ser. *75,* pp. 151-171, AGU, Washington DC, 1998.

Schodlok, M. P., C. B. Rodehacke, H. H. Hellmer, and A. Beckmann, Possible sources of the deep CFC maximum in the eastern Weddell Sea, *Geophys. Res. Let.*, in press.

H.H. Hellmer and A. Beckmann, Alfred-Wegener-Institute for Polar and Marine Research, Postfach 12 01 61, D-27515 Bremerhaven, Germany. (e-mail: hhellmer@awi-bremerhaven.de; beckmann@awi-bremerhaven.de)

(Received February 22, 2001; accepted May 7, 2001.)

Figure Captions

Figure 1. Annual mean (21^{st} model year) overturning transport streamfunction for the whole Southern Ocean south of 54°S as a function of latitude and density (σ_2). For densities $\sigma_2 \geq 37.1$ kg m^{-3} (dashed line), the vertical scale is stretched to better present the narrow dense water transports. The gray line marks the density $\sigma_2 = 37.16$ kg m^{-3} defined as upper bound for dense AABW formed south of the ACC [*Orsi et al.,* 1999]. Dashed contours indicate counter-clockwise, solid contours clockwise circulations (see arrows). Bold solid lines represent the minimum (upper) and maximum (lower) density value for each latitudinal band. Contour spacing is 2×10^6 m^{3}s^{-1} starting from $\pm1\times10^6$ m^{3}s^{-1}

Figure 1. Annual mean (21^{st} model year) overturning transport streamfunction for the whole Southern Ocean south of 54°S as a function of latitude and density (σ_2). For densities $\sigma_2 \geq 37.1$ kg m^{-3} (dashed line), the vertical scale is stretched to better present the narrow dense water transports. The gray line marks the density $\sigma_2 = 37.16$ kg m^{-3} defined as upper bound for dense AABW formed south of the ACC [*Orsi et al.,* 1999]. Dashed contours indicate counter-clockwise, solid contours clockwise circulations (see arrows). Bold solid lines represent the minimum (upper) and maximum (lower) density value for each latitudinal band. Contour spacing is 2×10^6 m^{3}s^{-1} starting from $\pm1\times10^6$ m^{3}s^{-1}

Figure 2. Annual mean (21^{st} model year) horizontal distribution of the near-bottom density field relative to 2000 m (σ_2) south of 50°S. Areas with densities higher (lower) than $\sigma_2 \geq 37.16$ kg m^{-3} are shaded dark gray (light gray). Superimposed is layer thickness with $\sigma_2 > 37.16$ kg m^{-3}; contour spacing is 500 m. WS=Weddell Sea, RS=Ross Sea, WAL=Wilkes-Adélie Land, PB=Prydz Bay, EL=Enderby Land.

Figure 2. Annual mean (21^{st} model year) horizontal distribution of the near-bottom density field relative to 2000 m (σ_2) south of 50°S. Areas with densities higher (lower) than $\sigma_2 \geq 37.16$ kg m^{-3} are shaded dark gray (light gray). Superimposed is layer thickness with $\sigma_2 > 37.16$ kg m^{-3}; contour spacing is 500 m. WS=Weddell Sea, RS=Ross Sea, WAL=Wilkes-Adélie Land, PB=Prydz Bay, EL=Enderby Land.

Figure 3. Same as Fig. 1 but devided in Atlantic (left) and Indian-Pacific (right) sectors south of 66°S. Since a sensible transport streamfunction calculation requires a coast-to-coast integration, the Atlantic sector extends from Enderby Land (50°E) to Antarctic Peninsula (60°W) while the Indian-Pacific sector encompasses the remaining Southern Ocean. This results in an Indian-Pacific coastline two-times longer than the Atlantic coast.

Figure 3. Same as Fig. 1 but devided in Atlantic (left) and Indian-Pacific (right) sectors south of 66°S. Since a sensible transport streamfunction calculation requires a coast-to-coast integration, the Atlantic sector extends from Enderby Land (50°E) to Antarctic Peninsula (60°W) while the Indian-Pacific sector encompasses the remaining Southern Ocean. This results in an Indian-Pacific coastline two-times longer than the Atlantic coast.

Figure 1

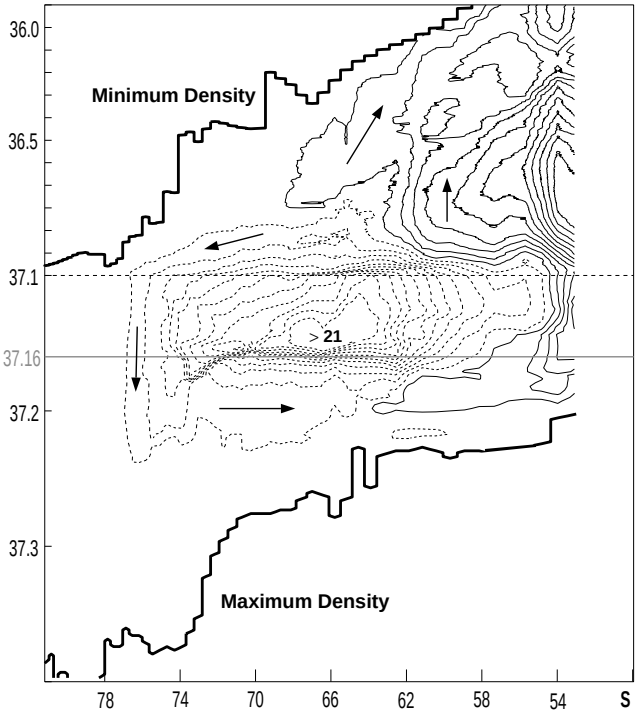
36.0
36.5
37.1
37.16
37.2
37.3
Minimum Density
> 21
Maximum Density
78
74
70
66
62
58
54
S

Figure 2

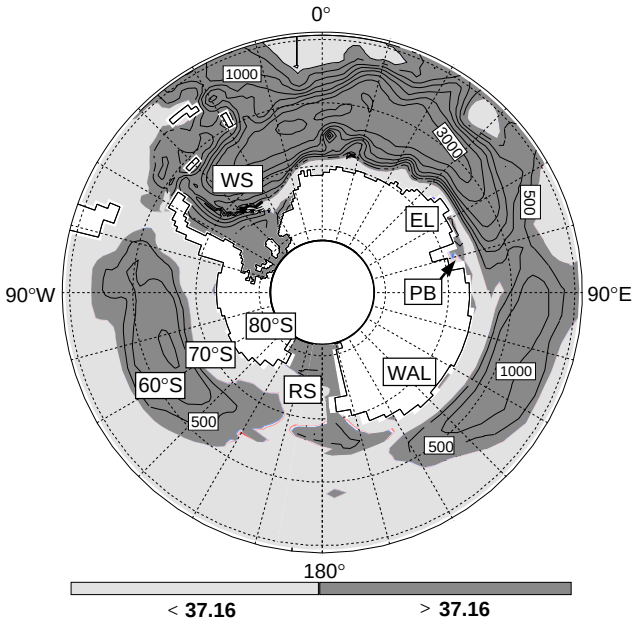
0°
90°W
90°E
180°
1000
3000
500
WS
EL
PB
80°S
70°S
60°S
RS
WAL
1000
500
500
< 37.16
> 37.16

Figure 3

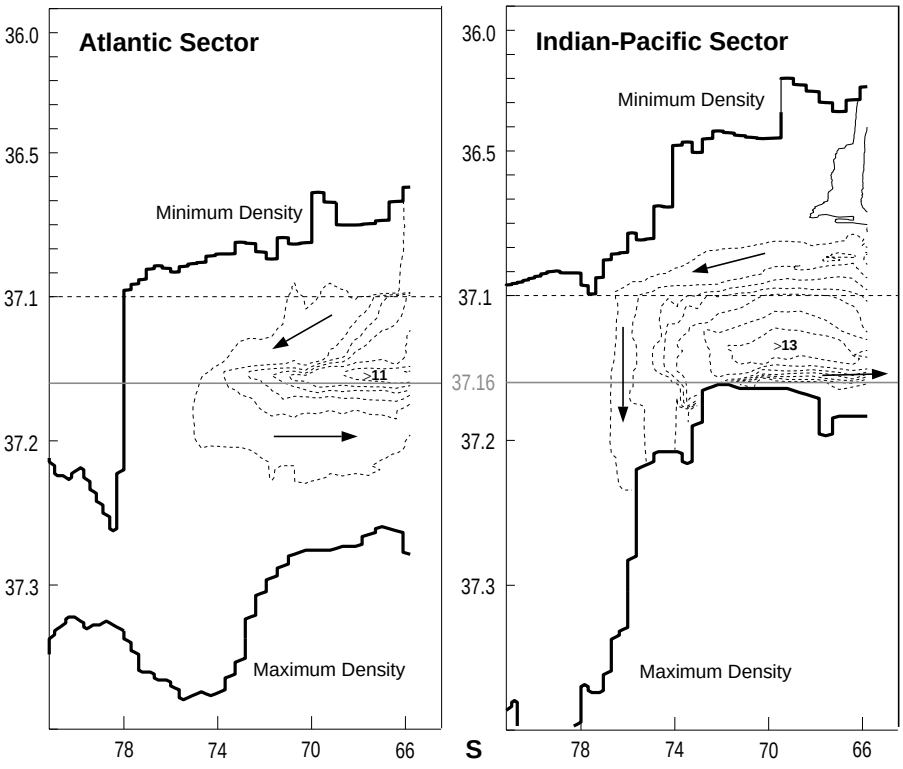
Atlantic Sector
Minimum Density
Maximum Density
>11
36.0
36.5
37.1
37.2
37.3
78
74
70
66
S
Indian-Pacific Sector
Minimum Density
Maximum Density
>13
37.16

HELLMER AND BECKMANN: SOUTHERN OCEAN BOTTOM WATER SOURCES

HELLMER AND BECKMANN: SOUTHERN OCEAN BOTTOM WATER SOURCES

HELLMER AND BECKMANN: SOUTHERN OCEAN BOTTOM WATER SOURCES

HELLMER AND BECKMANN: SOUTHERN OCEAN BOTTOM WATER SOURCES

HELLMER AND BECKMANN: SOUTHERN OCEAN BOTTOM WATER SOURCES

HELLMER AND BECKMANN: SOUTHERN OCEAN BOTTOM WATER SOURCES

HELLMER AND BECKMANN: SOUTHERN OCEAN BOTTOM WATER SOURCES

HELLMER AND BECKMANN: SOUTHERN OCEAN BOTTOM WATER SOURCES

HELLMER AND BECKMANN: SOUTHERN OCEAN BOTTOM WATER SOURCES

HELLMER AND BECKMANN: SOUTHERN OCEAN BOTTOM WATER SOURCES

HELLMER AND BECKMANN: SOUTHERN OCEAN BOTTOM WATER SOURCES

HELLMER AND BECKMANN: SOUTHERN OCEAN BOTTOM WATER SOURCES

HELLMER AND BECKMANN: SOUTHERN OCEAN BOTTOM WATER SOURCES

HELLMER AND BECKMANN: SOUTHERN OCEAN BOTTOM WATER SOURCES

HELLMER AND BECKMANN: SOUTHERN OCEAN BOTTOM WATER SOURCES

HELLMER AND BECKMANN: SOUTHERN OCEAN BOTTOM WATER SOURCES

HELLMER AND BECKMANN: SOUTHERN OCEAN BOTTOM WATER SOURCES

HELLMER AND BECKMANN: SOUTHERN OCEAN BOTTOM WATER SOURCES

HELLMER AND BECKMANN: SOUTHERN OCEAN BOTTOM WATER SOURCES

HELLMER AND BECKMANN: SOUTHERN OCEAN BOTTOM WATER SOURCES

HELLMER AND BECKMANN: SOUTHERN OCEAN BOTTOM WATER SOURCES

HELLMER AND BECKMANN: SOUTHERN OCEAN BOTTOM WATER SOURCES

HELLMER AND BECKMANN: SOUTHERN OCEAN BOTTOM WATER SOURCES

HELLMER AND BECKMANN: SOUTHERN OCEAN BOTTOM WATER SOURCES